Lower critical fields, critical currents, and flux creep in $Pb_2Sr_2R_{1-x}Ca_xCu_3O_{8+y}$ (R = Y,Dy) single crystals

V. V. Metlushko* and G. Güntherodt
2. Physikalishes Institut, Rheinisch-Westfälische Technische Hochschule Aachen, Templergraben 55, W-5100 Aachen, Germany

V. V. Moshchalkov* and Y. Bruynseraede
Laboratorium voor Vaste Stof-Fysika en Magnetisme, Katholieke Universiteit te Leuven, Celestijnenlaan 200D, B-3001 Leuven, Belgium

M. M. Lukina
Physics Department, Moscow State University, 117234, Moscow, Russia
(Received 8 October 1992)

The lower critical field $\mathbf{H}_{c1}(T)$, temperature and field dependences of the critical current $j_c(T,H)$, and the normalized magnetization relaxation rate $d(\ln M)/d(\ln t)$ have been studied for two orientations of the magnetic field $\mathbf{H}\|c$ and $\mathbf{H}\perp c$ in $Pb_2Sr_2R_{1-x}Ca_xCu_3O_{8+y}$ (R = Y,Dy) single crystals having practically a cubic shape with characteristic dimensions $0.6\times0.6\times0.5$ mm^3. $\mathbf{H}_{c1}(T)$ shows for $\mathbf{H}\|c$ a positive curvature with decreasing temperature without the usual low-temperature saturation found for the $\mathbf{H}\perp c$ orientation. This anomalous $\mathbf{H}_{c1}^{\|c}(T)$ behavior is related to the modification of the character of the field penetration in a layered structure consisting of a stack of superconducting and nonsuperconducting planes. The temperature dependence of the normalized relaxation rate $S=d(\ln M)/d(\ln t)$ shows a maximum at temperatures where the largest anisotropy of the critical currents is observed. Magnetic measurements have been used to obtain current-voltage characteristics from the damping electric field determined by the magnetic-flux creep rate. The analysis of $j_c(T,H)$, the temperature and field dependences of $d(\ln M)/d(\ln t)$, and of the $\mathbf{H}_{c1}(T)$ data shows that a continuous decoupling of the pancakelike vortices takes place with increasing temperature or magnetic field. A striking similarity between the temperature dependences of the normalized relaxation rate observed for $\mathbf{H}\|c$ and the $\mathbf{H}$ orientation very close to $\mathbf{H}\perp c$ implies that the flux-phase dynamics is mainly determined by the component of the applied magnetic field normal to the (a,b) planes, i.e., by the thermal activation of the motion of the pancake vortices in $Pb_2Sr_2R_{1-x}Ca_xCu_3O_{8+y}$. This material is of particular interest, because its anisotropic behavior is intermediate between that of $YBa_2Cu_3O_7$ and $Bi_2Sr_2CaCu_2O_x$ and its $T_c\approx80$ K is comparable to that of $Bi_2Sr_2CaCu_2O_x$.

I. INTRODUCTION

Among other high-T_c oxides, the recently discovered family of superconductors $Pb_2Sr_2R_{1-x}Ca_xCu_3O_{8+\delta}$ (Ref. 1) has not been studied in detail yet, which is mainly related to difficulties in obtaining relatively large high quality single crystals. As a result, only a few reported investigations[2–5] have been performed so far on single crystals. Reedyk *et al.*[4] studied temperature dependences of lower critical fields $H_{c1}(T)$ and London penetration depths $L(T)$. The characteristic scale for the flux-creep activation energy $U_0\approx20$–90 meV was obtained by Pradhan *et al.*[6] on a $Pb_2Sr_2Y_{1-x}Ca_xCu_3O_{8+\delta}$ single crystal with $T_c\approx35$ K, which is noticeably smaller than the highest possible T_c for this system, typically about 80 K.[1,2]

Using the flux growth method from the nonstoichiometric melts with an excess of PbO, SrO, and CuO (Ref. 2), we were recently able to obtain quite large high quality single crystals having an almost perfect cubic shape. To grow the crystals, the crucible was quickly heated up to 1030 °C, held at this temperature for 30 min and then cooled to 800 °C at 5 °C/h and to 550 °C at 20 °C/h. Then the crucible was cooled in the furnace in a flow of N_2 gas. The single crystals were carefully extracted from the flux and the composition determined by the x-ray microprobe using a JSM-820 Jeol electron microscope with an accuracy of $\pm0.1\%$. All measurements reported in the present paper have been carried out on the $Pb_{2.00}Sr_{2.00}R_{0.67}Ca_{0.33}Cu_{3.00}O_{8+\delta}$ (R = Y,Dy) single crystals with $T_c\approx80$ K and characteristic dimensions of $0.6\times0.6\times0.5$ mm^3. We have studied temperature, time, and field dependences of the magnetization M on a MPMS2 Quantum Design SQUID magnetometer[7] with the scan length 3 cm, corresponding to a field homogeneity of better than 0.05%.

II. LOWER CRITICAL FIELDS

As we have already mentioned, an almost cubic shape of the available single crystals makes them very suitable for studies of the anisotropy of different superconducting properties. The demagnetizing factor n_d calculated in the approximation of an inscribed ellipsoid[8–10] for our samples is nearly the same for both $\mathbf{H}\|c$ ($n_d\approx0.371$) and $\mathbf{H}\perp c$ ($n_d\approx0.315$) orientations. This difference in the

demagnetizing factors n_d ($H\|c$) and n_d ($H\perp c$) is much smaller than that for typical plateletlike high-T_c crystals.

Temperature dependences of the magnetic moment $P_m = MV$ of $Pb_2Sr_2Y_{1-x}Ca_xCu_3O_{8+\delta}$, where M is the magnetization and V is the volume of the crystal, are given in Fig. 1 for $\mathbf{H}=10$ G. We note that all magnetic data are presented throughout this paper in P_m vs $T,\mathbf{H}$ plots rather than in M vs $T,\mathbf{H}$ curves to exclude an additional error in M appearing because of uncertainties in the volume determination. The P_m vs T curve (Fig. 1) shows a sharp superconducting transition with the same transition temperature $T_c \approx 80$ K for the two systems $Pb_2Sr_2Y_{1-x}Ca_xCu_3O_{8+\delta}$ (PSYCCO), see Fig. 1 and $Pb_2Sr_2Dy_{1-x}Ca_xCu_3O_{8+\delta}$ (PSDCCO), see Fig. 2(a). The lower the applied magnetic field, the sharper the superconducting transition. As in all other known high-T_c oxides, the saturation value of P_m at $T\rightarrow 0$ is much smaller for the Meissner field-cooled (FC) than for the shielding zero-field-cooled (ZFC) measurements.

The magnetization of single crystals with Dy consists of two contributions arising from the diamagnetic response of the superconducting state and the paramagnetic response form the rare-earth Dy^{3+} ions. The latter is strongly field and temperature dependent. In high fields and at lower temperatures, the paramagnetic response dominates over the diamagnetic one as shown in Fig. 2(b), where the resulting $P_m^{FC}(T)$ curve measured for $\mathbf{H}=535.6$ G lies (for $T \le T_c$) completely in the paramagnetic region [Fig. 2(b)]. The paramagnetic component can be fitted by a Curie-Weiss dependence $M \approx \text{const}/(T+\Theta)$ with a parameter $\Theta \approx -3$ K in qualitative agreement with the effective magnetic moment of an isolated Dy^{3+} ion.

A detailed analysis of the $P_m^{FC}(T)$ data is presented in Fig. 3 where a strong field dependence of the Meissner fraction is demonstrated for both $\mathbf{H}\|c$ and $\mathbf{H}\perp c$ field orientations. The effective magnetic field $\mathbf{H}_{\text{eff}}$ has been calculated by taking into account the demagnetizing fields.

The drastic suppression of the Meissner fraction by an applied field implies that in order to obtain the full 100% Meissner effect, very low fields (less than 10^{-2} G[11–13]) must be used.

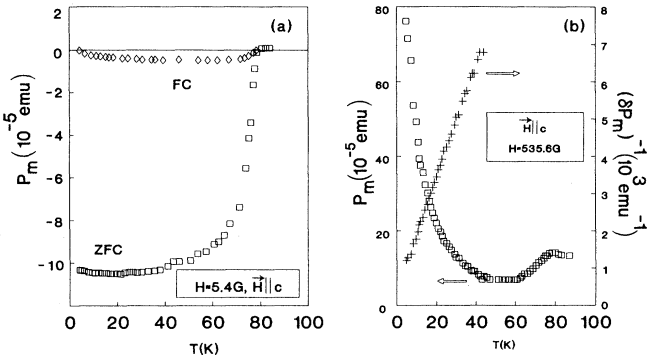

FIG. 2. (a) Temperature dependence of the magnetic moment P_m of a $Pb_2Sr_2Dy_{1-x}Ca_xCu_3O_{8+y}$ single crystal ($\mathbf{H}\|c$):□=ZFC, ◇=FC. (b) Temperature dependence of P_m^{FC} and $(dP_m^{FC})^{-1}$ of a $Pb_2Sr_2Dy_{1-x}Ca_xCu_3O_{8+y}$ single crystal, $\mathbf{H}=535.6$ G, $\mathbf{H}\|c$.

The magnetic moment vs field curves measured at different fixed temperatures have been used to determine the lower critical field. For this purpose we subtracted first the ideal linear contribution corresponding to the full diamagnetic response. Then the resulting difference δP_m is analyzed by the extrapolation method[14,15] which is based on the simple behavior $\delta P_m \sim (\mathbf{H}-\mathbf{H}_{c1})^2$, useful for practical purposes in finding $\mathbf{H}_{c1}$ as the field where the linear $(\delta M)^{1/2}$ vs $\mathbf{H}$ dependence intersects the $\mathbf{H}$ axis of the $(\delta P_m)^{1/2}$ vs $\mathbf{H}$ plot (Fig. 4). For a slab with thickness d or a cylinder with radius R, the following relation between δM and $\mathbf{H}$ is valid[14]

$$\delta M = \frac{(\mathbf{H}-\mathbf{H}_{c1})^2}{2(\mathbf{H}^*-\mathbf{H}_{c1})} + \frac{(\mathbf{H}-\mathbf{H}_{c1})^3}{4(\mathbf{H}^*-\mathbf{H}_{c1})^2} + \frac{2\mathbf{H}_{c1}(1-m_{\text{eq}})(\mathbf{H}-\mathbf{H}_{c1})}{(\mathbf{H}^*-\mathbf{H}_{c1})}, \quad (1)$$

where $\mathbf{H}^* = \pi j_c d/5$ for a slab and $\mathbf{H}^* = 4\pi j_c R/10$ for a cylinder and $0 \le m_{\text{eq}} \le 1$. The extrapolation method may be used in this form when the field dependence of critical

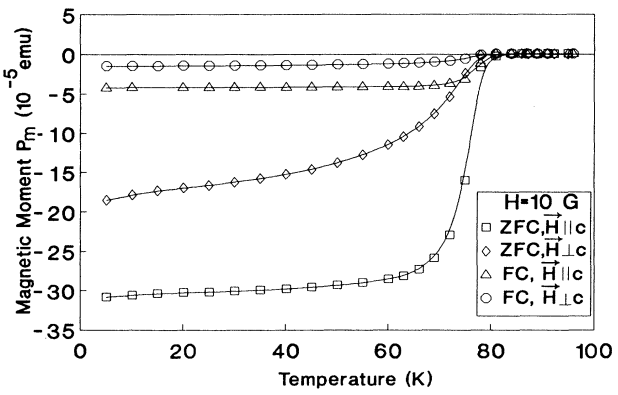

FIG. 1. Temperature dependence of the magnetic moment P_m of a $Pb_2Sr_2Y_{1-x}Ca_xCu_3O_{8+y}$ single crystal, $\mathbf{H}=10$ G: □=ZFC, $\mathbf{H}\|c$, △=FC, $\mathbf{H}\|c$, ◇=ZFC, $\mathbf{H}\perp c$, ○=FC, $\mathbf{H}\perp c$.

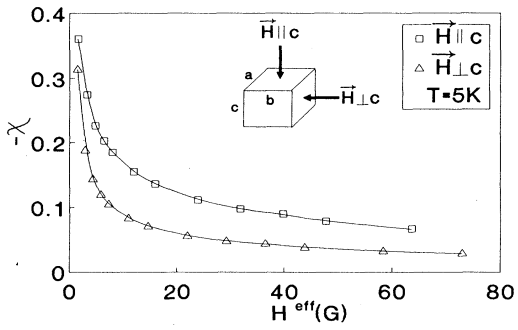

FIG. 3. Field dependence of the Meissner phase of a $Pb_2Sr_2Y_{1-x}Ca_xCu_3O_{8+y}$ single crystal at 5 K: □=$\mathbf{H}\|c$, △=$\mathbf{H}\perp c$.

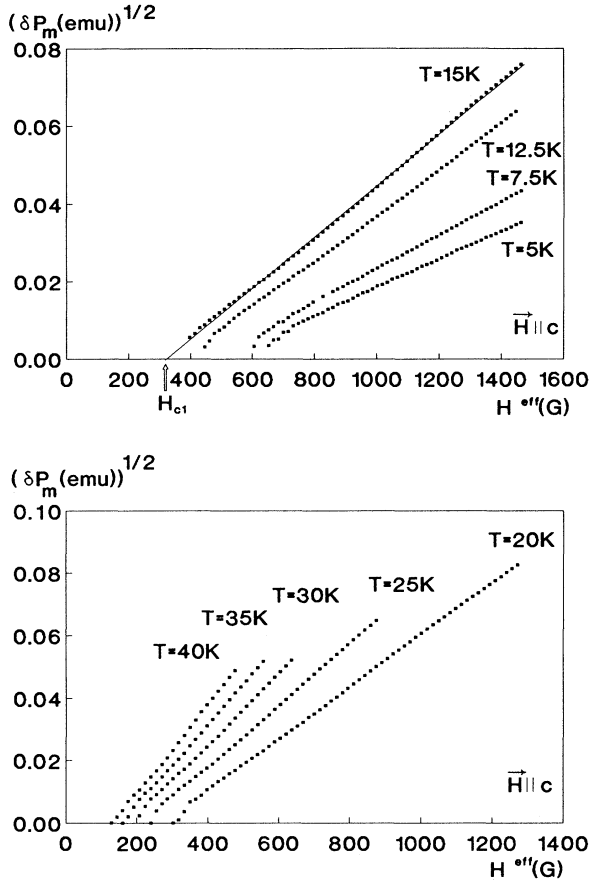

FIG. 4. $\delta P_m^{1/2}$ vs the demagnetization-corrected field $\mathbf{H}_{\rm eff}\mathbf{H}\|c$ for $Pb_2Sr_2Y_{1-x}Ca_xCu_3O_{8+y}$

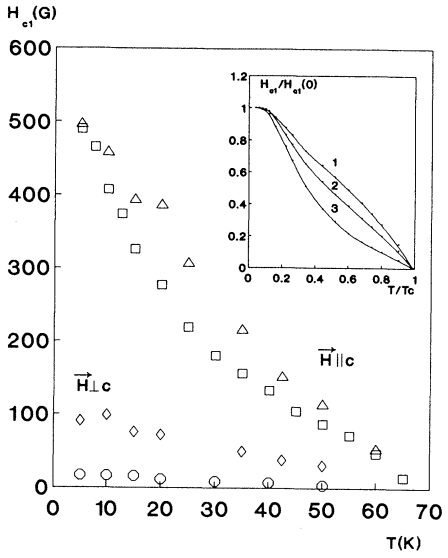

FIG. 5. Temperature dependence of the low critical field $\mathbf{H}_{c1}$ of a $Pb_2Sr_2Y_{1-x}Ca_xCu_3O_{8+y}$ single crystal: $\square=\mathbf{H}\|c$, $\circ=\mathbf{H}\perp c$ ($\triangle=\mathbf{H}\|c$ and $\Diamond=\mathbf{H}\perp c$ data taken from Reedyk *et al.* in Ref. 4). Inset: $\mathbf{H}_{c1}(T)$ curves calculated for S-N-S multilayers with different weight coefficient σ of N layers (curve $1-\sigma=5$, $2-\sigma=10$, $3-\sigma=100$) (data taken from Golubov *et al.* in Ref. 28).

current $j_c(\mathbf{H})$ is negligible and the second term in Eq. (1) is much smaller than the first one. As it is illustrated in Fig. 4, a good linearity of $(\delta M)^{1/2}$ vs $\mathbf{H}_{\rm eff}$ is clearly seen for $\mathbf{H}\|c$ in a wide range of fields and temperatures. For $\mathbf{H}\perp c$, the $(\delta M)^{1/2}$ vs $\mathbf{H}_{\rm eff}$ curve has a more complicated shape, indicating the importance of the second term in Eq. (1).

Figure 5 shows temperature dependences of lower critical fields obtained by the extrapolation method. We should note here that our $\mathbf{H}_{c1}^{\perp c}(T)$ data give the highest possible estimate of $\mathbf{H}_{c1}^{\perp c}$, which means that the real $\mathbf{H}_{c1}^{\perp c}$ values might be even lower. For the $\mathbf{H}\|c$ orientation there is a good agreement of our $\mathbf{H}_{c1}^{\|c}(T)$ data with those reported earlier by Reedyk *et al.*[4] which are also displayed in Fig. 5, with $\mathbf{H}_{c1}^{\|c}(0)\approx 500$ G. For the $\mathbf{H}\perp c$ case, we have obtained systematically lower $\mathbf{H}_{c1}$ values, compared to Ref. 4, with $\mathbf{H}_{c1}^{\perp c}(0)\approx 16$ G. The anisotropy parameter

$$\Gamma\equiv(m_c/m_{ab})^{1/2}=\mathbf{H}_{c1}^{\|c}/\mathbf{H}_{c1}^{\perp c}=L_c/L_{ab}\geq 31$$

gives the effective-mass ratio $m_c/m_{ab}\geq 960$, indicating a well-defined regime of a weak coupling between superconducting CuO_2 bilayers along the c axis. The quasi-two-dimensional (2D) character of high-T_c oxides has been emphasized before for $Bi_2Sr_2CaCu_2O_y$ ($\Gamma\approx 50-140$),[16,17] $Tl_2Ba_2CaCu_2O_x$ ($\Gamma\approx 70$),[18] and for $YBa_2Cu_3O_z$ ($\Gamma\approx 5$).[19-21]

The anomalous temperature dependence of $\mathbf{H}_{c1}^{\|c}(T)$ is also a signature of the layered structure of high-T_c oxides, which may be effectively treated as S-N-S or S-I-S multilayers with the superconducting CuO_2 layer separated by nonsuperconducting layers.[22-28] The contribution arising from these layers leads to an appearance of a positive $\mathbf{H}_{c1}(T)$ curvature at low temperatures. We have made a qualitative comparison of our measured $H_{c1}^{\|c}(T)$ curve with the model calculation[28] for the S-N-S multilayers (see inset of Fig. 5). The theoretical fit may describe an anomalous positive curvature of $\mathbf{H}_{c1}^{\|c}(T)$, though the constraints used in Ref. 28 might not be suitable for the case of high-T_c materials, where the space layers may be insulating.

Due to ambiguities in the determination of $\mathbf{H}_{c1}^{\perp c}(T)$, we are not discussing the $\mathbf{H}_{c1}^{\perp c}(T)$ dependence given in Fig. 5 and also its difference with the data reported by Reedyk *et al.*[4] Nevertheless, we are sure that our data give only an *upper* limit for $\mathbf{H}_{c1}^{\perp c}(T)$, i.e., the real anisotropy may be, in fact, even essentially higher than $\Gamma=31$ mentioned above.

Having an anisotropic ($\Gamma\geq 31$) superconducting sample with practically a cubic shape, it was interesting to check experimentally the theoretical calculation[29-32] for the field dependences of the magnetic moment for different angles between $\mathbf{H}$ and the c axis. Plotting the reversible part of the magnetic moment for $\mathbf{H}\perp c$ vs $\mathbf{H}$ (Fig. 6), we clearly see the presence of the two maxima, in

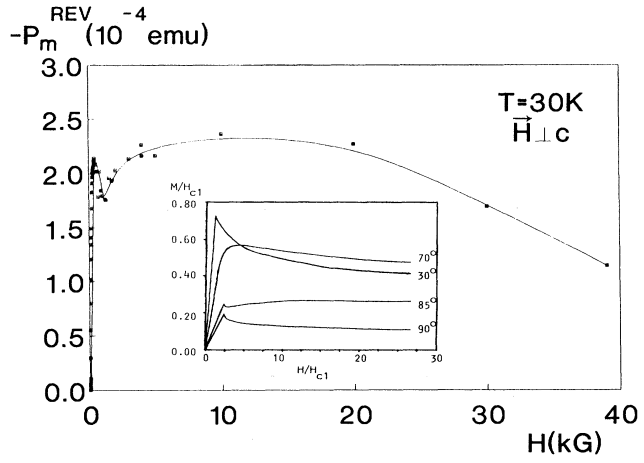

FIG. 6. Field dependence of the reversible magnetic moment P_m^{REV} of a $Pb_2Sr_2Y_{1-x}Ca_xCu_3O_{8+y}$ single crystal, **H** near **H**$\perp c$ direction, $T=30$ K. Inset: Full magnetic moment M vs external magnetic field **H** for various angles Θ_v in an ellipsoidal sample of a layered superconductor (data taken from Buzdin *et al.* in Ref. 30), where Θ_v is the angle between the c axis and the field direction.

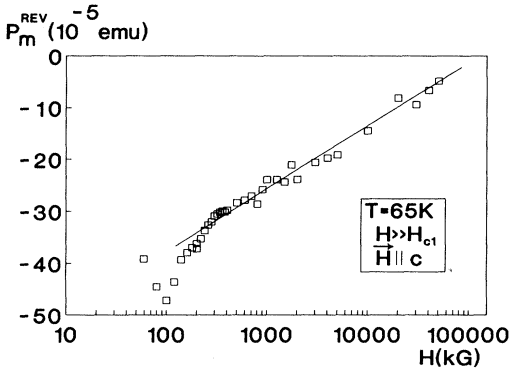

FIG. 7. Field dependence of the reversible magnetic moment P_m^{REV} of a $Pb_2Sr_2Y_{1-x}Ca_xCu_3O_{8+y}$ single crystal, **H**$\|c$, $T=65$ K.

correspondence with the theoretical $P_m(\mathbf{H})$ data for $\Theta_v=85°$, i.e., for small tilt angles $\alpha=(\pi/2)-\Theta_v=5°$, where Θ_v is an angle between the vortex lattice and the c axis.[30] From this point of view, the real **H** orientation in our experiment seems to deviate by an angle of $\alpha\sim 5°$ from the CuO_2 planes. For tilted fields this results in[31]

$$\mathbf{H}_{c1}^{\perp c}\text{ "measured"}=\mathbf{H}_{c1}^{\perp c}+\frac{\mathbf{H}_{c1}^{\|c}}{\cos\Theta_v}\ ,$$

and the difference between our estimates for $\mathbf{H}_{c1}^{\perp c}$ (Fig. 5) and Reedyk's data[4] may be easily explained as originating mainly from a small misorientation, which, however, might be very important for strongly anisotropic superconductors.

Field dependences of the magnetic moment $P_m(\mathbf{H})$ can be decomposed into two parts corresponding to reversible (P_m^{REV}) and irreversible terms (P_m^{IRR}):[33–36]

$$P_m^{REV}(\mathbf{H})=\tfrac{1}{2}[P_m^{+}(\mathbf{H})+P_m^{-}(\mathbf{H})]\ , \tag{2}$$

$$P_m^{IRR}(\mathbf{H})=\tfrac{1}{2}[P_m^{+}(\mathbf{H})-P_m^{-}(\mathbf{H})]\ , \tag{3}$$

where $P_m^{+}(\mathbf{H})$ and $P_m^{-}(\mathbf{H})$ are the upper and lower branches of hysteresis loops, respectively. The reversible contribution arises from the vortex lattice magnetization and it can be used to derive the temperature dependence of the penetration depth L. The Ginzburg-Landau (GL) analysis gives for the anisotropic 3D superconductors the following relation:[37]

$$M^{\|c}=\frac{\Phi}{32\pi^2L_{ab}^2}\ln\left[\frac{\mathbf{H}^{\|c}}{\mathbf{H}_{c2}^{\|c}\beta}\right]\ , \tag{4}$$

where Φ is the flux quantum, L_{ab} is the a,b-plane penetration depth, and β is a constant. The theory of the Josephson-coupled quasi-2D layered superconductors predicts for the **H** orientations not too close to **H**$\|ab$ a similar relation for the magnetization component perpendicular to the (a,b) plane:[32]

$$M^{\|c}=-\frac{\Phi}{16\pi^2L_{ab}{}^2}\left[\ln\left[\frac{\eta H_{c2}^{\|c}}{H^{\|c}}\right]^{1/2}+\alpha_{2D}\right]\ , \tag{5}$$

where α_{2D} is a vortex core contribution and η is a constant of order 1 for a hexagonal lattice. Using Eq. (4), we calculated the temperature variation of L_{ab}, which can be deduced from Fig. 7. By plotting P_m vs ln**H**, we see that there is a wide range of fields where Eqs. (4) and (5), predicting a P_m vs ln**H** relation, are fulfilled. The slope $dP_m/d(\ln\mathbf{H})$ gives $L_{ab}^{-2}(T)$ (see Fig. 8), which follows a BCS-like behavior (solid line in Fig. 8 and dashed lines in Fig. 9). The difference between our data (open circles, Fig. 9) and those reported by Reedyk *et al.*[4] (open squares, Fig. 9) is eliminated after the proper normalization by the different T_c values ($T_c\approx 80$ K, Fig. 1 and $T_c\approx 75$ K, Ref. 4). We have obtained the zero-

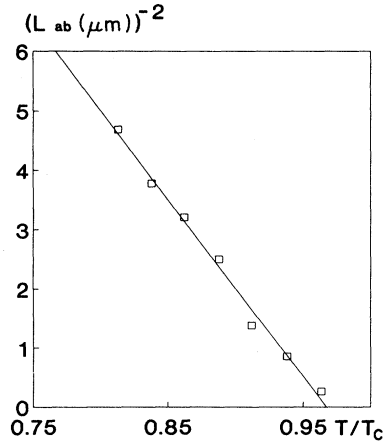

FIG. 8. L_{ab}^{-2} vs normalized temperature for $Pb_2Sr_2Y_{1-x}Ca_xCu_3O_{8+y}$, **H**$\|c$ where L_{ab} is the penetration depth of the a,b plane.

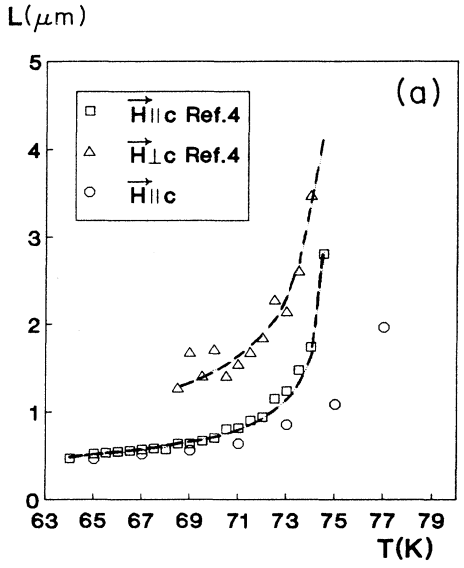

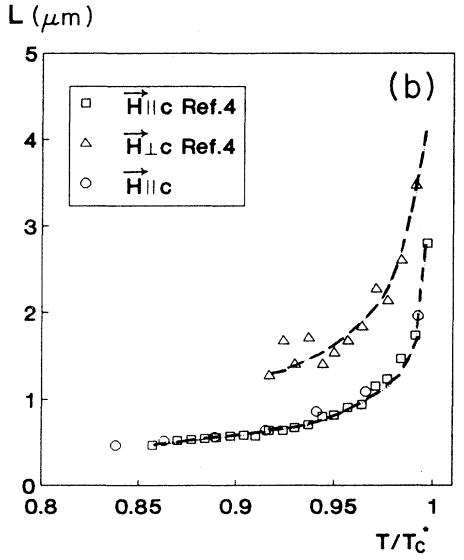

FIG. 9. Temperature dependence of the penetration depth L of a $Pb_2Sr_2Y_{1-x}Ca_xCu_3O_{8+y}$ single crystal $\circ = \mathbf{H} \| c$ ($\square = \mathbf{H} \| c$ and $\triangle = \mathbf{H} \perp c$ data taken from Reedyk *et al.* in Ref. 4).

temperature penetration depth in the *ab* plane $L_{ab}(0) = 1860$ Å, which is in agreement with $L_{ab}(0) = 2575$ Å (Ref. 4) and not far from the $L_{ab}(0)$ value in $YBa_2Cu_3O_x$ [$L_{ab}(0) = 1300-1700$ Å (Refs. 14, 38, and 39)] and $Bi_2Sr_2CaCu_2O_y$ [$L_{ab}(0) = 3000$ Å (Ref. 40)].

III. CRITICAL CURRENTS

The irreversible part of the magnetization [Eq. (3)] determines the behavior of the critical currents j_c. For $\mathbf{H} \| c$, the correspondence between j_c and the width of hysteresis loops is given by the isotropic Bean model,[34,35]

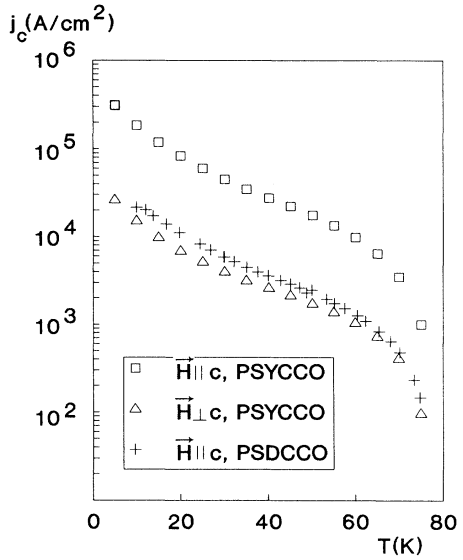

FIG. 10. Temperature dependence of the critical current j_c at $\mathbf{H}=0$ for: $\square = Pb_2Sr_2Y_{1-x}Ca_xCu_3O_{8+y}$, $\mathbf{H} \| c$, $\triangle = Pb_2Sr_2Y_{1-x}Ca_xCu_3O_{8+y}$, $H \perp c$, $+ = Pb_2Sr_2Dy_{1-x}Ca_xCu_3O_{8+y}$, $\mathbf{H} \| c$.

whereas for $\mathbf{H} \perp c$ the derivation of j_c should be based on the anisotropic Bean model.[36] This procedure has been used to find the $j_c(\mathbf{H}, T)$ dependences. Figure 10 shows the zero-field temperature variation of j_c of PSYCCO for both $\mathbf{H} \| c$ and $\mathbf{H} \perp c$ orientations and compares it with PSDCCO for $\mathbf{H} \| c$. The $j_c(T)$ curve is characterized by a quasi-exponential dependence observed previously in other high-T_c oxides (see Fig. 11). However, there is a noticeable change of the $j_c(T)$ slope around $T^{cr} \approx 15-20$ K ($T/T_c \approx 0.25$) which occurs continuously in $YBa_2Cu_3O_x$ [Fig. 11(a)][41-43] and in $Pb_2Sr_2R_{1-x}Ca_xCu_3O_{8+y}$ (Fig. 10), but abruptly in $Bi_2Sr_2CaCu_2O_y$[44-46] [Fig. 11(a)]. As was suggested before,[47] this type of anomaly seems to be

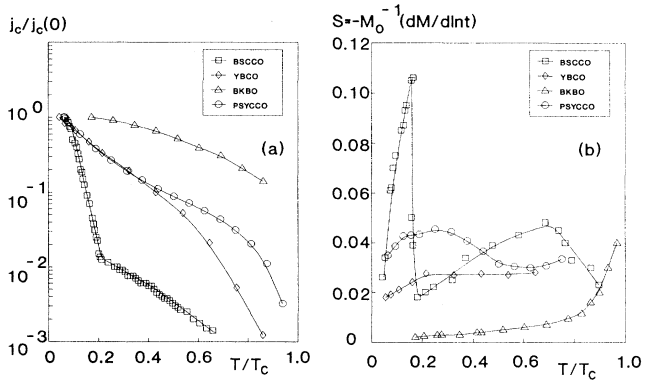

FIG. 11. (a) Temperature dependence of the critical current: $\square = Bi_2Sr_2CaCu_2O_x$ (Ref. 44), $\diamond = YBa_2Cu_3O_y$ (Ref. 41), $\triangle = Ba_{1-x}K_xBiO_3$ (Ref. 54), $\circ = Pb_2Sr_2Y_{1-x}Ca_xCu_3O_{8+y}$. (b) The temperature dependence of the normalized relaxation rate S: $\square = Bi_2Sr_2CaCu_2O_x$ (Ref. 44), $\diamond = YBa_2Cu_3O_y$ (Ref. 41), $\triangle = Ba_{1-x}K_xBiO_3$ (Ref. 54), $\circ = Pb_2Sr_2Y_{1-x}Ca_xCu_3O_{8+y}$.

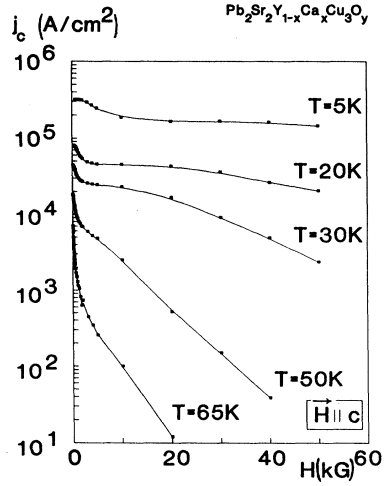

FIG. 12. Field dependence of the critical current of $Pb_2Sr_2Y_{1-x}Ca_xCu_3O_{8+y}$, $\mathbf{H}\|c$ at various temperatures.

caused by the crossover from the classical Abrikosov vortex lattice with pinning of straight flux lines by individual pinning centers at low temperatures to the new regime of collective pinning arising from decoupled quasi-2D pancake vortices, taking advantage of pinning by neighboring pinning centers in each plane. In this case, because of a weak coupling between superconducting planes, the flux line becomes more flexible to be pinned by many pinning centers in different decoupled CuO_2 planes, although these centers do not form a straight line parallel to $\mathbf{H}$. The crossover from individual to collective pinning leads to an enhancement of j_c which is evidenced by the decrease of the dj_c/dT slope around T^{cr} [see Figs. 10 and 11(a)]. A similar j_c enhancement caused by the change of the pinning mechanism is also observed when the temperature is held fixed and instead the applied field is varied[47–53] (Fig. 12). From this point of view, the field-induced decoupling of the pancake vortices[47] may explain the appearance of the so-called "peak effect" (Ref. 51) in high-T_c oxides, when j_c becomes larger with increasing field, forming a fishtail shape[50,51] or butterflylike[52] hysteresis loop.

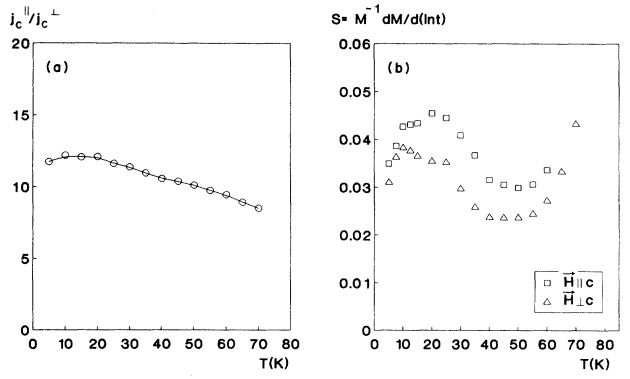

FIG. 13. (a) Temperature dependence of the critical current anisotropy $j_c^{\|}/j_c^{\perp}$ for a $Pb_2Sr_2Y_{1-x}Ca_xCu_3O_{8+y}$ single crystal. (b) Temperature dependence of the normalized relaxation rate $S=M_0^{-1}dM/d(\ln t)$ of a $Pb_2Sr_2Y_{1-x}Ca_xCu_3O_{8+y}$ single crystal: $\square=\mathbf{H}\|c$, $\triangle=\mathbf{H}\perp c$.

The anisotropy of critical currents $K_j=j_c^{\|}/j_c^{\perp}$ determined from magnetization data for $\mathbf{H}=0$ is slowly changing with temperature [Fig. 13(a)] and it has a maximum $K_j\approx 12$ at a temperature close to T^{cr}. At the same temperature the normalized relaxation rate $S=d(\ln M)/d(\ln t)$ [Fig. 13(b)] also exhibits a maximum. The details of the $S(T)$ behavior will be discussed below.

IV. FLUX CREEP

To get an idea to what extent the temperature variation of critical current is related to the change of the pinning potential U_0, we have also studied the relaxation of the magnetic moment, thus deriving from these data the information about the U_0 vs T dependences. Flux-creep processes were studied in the regime of the remanent magnetization measured after applying a magnetic field $\mathbf{H}=20$ kG, which is larger than the characteristic field $\mathbf{H}^*$ (Ref. 35) of the onset of the full field penetration for both orientations of $\mathbf{H}$.

The time dependences of P_m follow a logarithmic decay law, at least in the interval $t=10^2$–4×10^3 s used in our experiments. To separate the temperature variation of U_0 from the $j(T)$ dependence, it is important to use the normalized relaxation rate $S=(1/M_0)dM/d(\ln t)$, where M_0 is the initial magnetization value. The S vs T curve has a N-like shape with the maximum at $T=T^{CR}\approx 12$ K [Fig. 13(b)]. We should note here that the unusual N shape of the $S(T)$ dependence is now widely discussed in the literature. To compare the temperature variation of the normalized relaxation rate $S(T)$ in different oxide superconductors, we have plotted in Fig. 11 the $j_c(T)$ and $S(T)$ data for $Ba_{1-x}K_x$ BiO_3 (BKBO),[54] $YBa_3Cu_3O_x$ (YBCO),[41,54–57] $Bi_2Sr_2CaCu_2O_y$ (BSCCO),[44–46] and PSYCCO. In isotropic cubic BKBO, superconductors $j(T)$ and $S(T)$ are monotonous functions of temperature, with the smaller $j_c(T)$ values at high temperatures [Fig. 11(a)] being in a correspondence with the larger $S(T)\sim 1/U_0(T)$ values [see Eq. (6) and Fig. 11(b)]. In layered YBCO, BSCCO, and PSYCCO superconductors, the situation concerning $S(T)$ and $j_c(T)$ is more complicated. In quasi-2D BSCCO and also in $Tl_2Ba_2Ca_2Cu_3O_x$ (Ref. 58), there is a kink in the $j_c(T)$ dependence at $T=T^{CR}$ (Ref. 59) see Fig. 11(a), which is accompanied by a sharp suppression of the $S(T)$ values at the same temperature $T=T^{CR}$;[44–46,58] see Fig. 11(b). In YBCO superconductors there is a wide plateau on the $S(T)$ curve [Fig. 11(b)], which is related to the modification of the exponential variation of j_c in the same temperature range. The $j_c(T)$ and $S(T)$ dependences for PSYCCO (Fig. 11) look like an intermediate case between quasi-2D BSCCO and strongly 3D-like YBCO. The plateaulike dependence of $S(T)$ is quite often considered[41,54–57] as evidence for the existence of the vortex glass phase.[59,60]

Usually the magnetization relaxation process is caused

by the thermal excitation of a vortex line over a characteristic potential barrier U_0.[61] This process also leads to a decrease of j_c (Ref. 62) and the normalized relaxation rate $S(T)$ is determined by[63,64]

$$S(T)=-\frac{kT}{U_0-kT\ln(t/\tau_{\text{eff}})} . \tag{6}$$

There are two well-known relations available between the pinning potential U_0 and the critical current. In the Anderson model[61] we have

$$U(j)=U_0(1-j/j_{c0}) , \tag{7}$$

whereas in the Zeldov model[65,66] a logarithmic relation holds:

$$U(j)=U_0\ln(j_{c0}/j) . \tag{8}$$

The simple substitution of $U(j)$ into Eq. (6) shows that neither Anderson's[61] nor Zeldov's[65,66] model can interpret successfully the experimentally observed $S(T)$ plateau, since both models predict an *upward* $S(T)$ curvature which at most corresponds to the isotropic BKBO case but not to the $S(T)$ behavior in layered high-T_c oxides [Fig. 11(b)].

In the framework of the collective pinning[67,68] and vortex glass[59,60] models, we have

$$U(j)=\frac{U_0(T)}{\mu}\left[\left[\frac{j_{c0}(T)}{j}\right]^{\mu}-1\right] \tag{9}$$

and

$$\begin{aligned} j_{c0}(T)&=j_{c00}\left[1-\left[\frac{T}{T_c}\right]^2\right]^n , \\ U_0(T)&=U_{00}\left[1-\left[\frac{T}{T_c}\right]^2\right]^n , \end{aligned} \tag{10}$$

where μ and n are constants. It is possible to obtain a plateaulike $S(T)$ dependence,[62] though the fitting procedure involves quite a large number of fitting parameters. We should not be very enthusiastic at this point, however, since our experimental data for PSYCCO convincingly demonstrate that with the increasing decoupling between CuO_2 superconducting planes, the plateaulike $S(T)$ dependence is transformed into the N-like $S(T)$ curve [Fig. 11(b)] with a maximum at $T=T^{\text{CR}}\approx 10-20$ K. Moreover, in quasi-2D BSCCO superconductors this maximum becomes much sharper, with a drop of $S(T)$ by a factor of 6–10 (Refs. 44–46) in a very narrow (≤ 2 K) temperature interval. The observation of a very sharp drop of $S(T)$ at $T=T^{\text{CR}}\approx 15$ K in BSCCO made it necessary to put forward an idea about changing to a new pinning mechanism at $T\geq T^{\text{CR}}$ (Refs. 44 and 46).

Summing up this section, we note that a continuous decoupling of the superconducting CuO_2 planes results in a strong modification of the $S(T)$ dependences with increasing temperature from a monotonously growing $S(T)$ in cubic BKBO (Ref. 54) compounds through intermediate plateaulike (YBCO) and N-like (PSYCCO) $S(T)$ curves to a sharp low-temperature anomaly in quasi-2D BSCCO superconductors.[44–46] The proper theoretical description of the whole range of the $S(T)$ behavior in layered superconductors with a varying degree of decoupling between superconducting planes is still lacking. We may only suggest here that the sharp low-temperature $S(T)$ maximum, which seems to be *not* reproduced by either vortex glass[59,60] or by collective pinning[67,68] models, appears to be due to an abrupt onset of a different pinning regime (Fig. 11). This speculative idea is also supported by the observation of the pronounced kink in the $j_c(T)$ dependence at $T=T^{\text{CR}}$ [Fig. 11(a)]. One of the possible scenarios for a change of the pinning mechanism was proposed by Fisher *et al.*[59] In layered superconductors at low temperatures and in low fields, the interlayer coupling is playing a more dominant role, resulting in a 3D behavior, though strongly anisotropic. With increasing temperature, the crossover from 3D vortex lines to quasi-2D pancakelike vortices occurs, and in each CuO_2 superconducting plane the pancakelike vortices can take advantage of being decoupled from other vortices to move to available neighboring pinning centers to optimize their pinning potential. In this case, the full vortex line, consisting of all pancakelike independent vortices sitting one underneath the other in different superconducting CuO_2 planes, is sufficiently flexible to realize a higher total effective pinning potential U_0 and, consequently, a smaller S value. Such a crossover should be accompanied by the appearance of a power-law behavior of the current-voltage (I-V) characteristics.

Current-voltage characteristics can be successfully used for studies of the dissipation processes in type II superconductors. Within the framework of the Kim-Anderson model,[61] the flux creep leads to a finite dissipation corresponding to the existence of the finite resistance:

$$R_L\equiv\lim_{I\to 0}\frac{V}{I} ,$$

which is a linear function of temperature T with the zero resistance state being realized only at $T=0$.[69] Recently new possible flux phases have been proposed by Fisher *et al.*,[59,60] including the vortex glass (VG) phase with the frozen positions of the individual flux lines. These restrictions for the flux motion are also accompanied by a weaker dissipation which results in a power law for the current-voltage characteristics for D-dimensional samples:[59,60]

$$E(j,T=T_g)=j^{(Z+1)/(D-1)} , \tag{11}$$

where j is the current density, E is the electric field, and T_g is the phase-transition temperature. For $T<T_g$, according to the VG theory, a *negative* curvature of the I-V curves should be seen on the log$I$-log$V$ plot, in contrast to the *positive* curvature expected from the Anderson-Kim flux-creep model with $V\propto\sinh(I/I_0)$.[61] From this point of view, the change of curvature of the log$I$-log$V$ plot may be interpreted as an indication of the transition into the vortex phase.

Conventional methods of the I-V measurements are limited by poor voltage resolution. On the other hand, the derivation of the voltage from the flux-creep data[70–72] has an advantage of making available the pico-

volt range for current-voltage characteristic studies. The underlying idea is quite simple. The shielding current itself can easily be found from the corresponding width of the magnetic-moment hysteresis loop, while the electric field E may be obtained on the basis of the Faraday induction law

$$E=\frac{1}{2\pi R}\frac{d\Phi}{dt}=\frac{3\mu_0 I}{2\pi^2 R^2}\frac{dP_m}{dt}\ , \tag{12}$$

where P_m and R are the magnetic moment and the radius of the sample, respectively, and $I=3.328$ (Refs. 73,74).

As in classical type II superconductors, e.g., Nb-Ti and Nb_3Sn, where $V=kI^n$, with $n=15-150$ (Ref. 75), we have also found quite large n values for the PSYCCO single crystals: $n\sim 25-45$. All our flux-creep measurements have been done in the regime of the critical state, i.e., when the applied magnetic field $\mathbf{H}=2T$ was much higher than the field $\mathbf{H}^*$ of the onset of the full field penetration. The I-V curves (Fig. 14) follow the power law

$$E=E_0(j/j_0)^n\ , \tag{13}$$

with the exponent n being strongly suppressed by magnetic field. We have also tried to fit an exponential relation between j and E as predicted in Ref. 61, but under these conditions the fitting gets worse. For long enough times ($t\geq 100$ s) the n value in the power law [Eq. (13)] is inversely proportional to the normalized relaxation rate:[73,74]

$$n=\frac{d(\ln E)}{d(\ln j)}=\left[\frac{d(\ln P_m)}{d(\ln t)}\right]^{-1}=\frac{1}{S}\ . \tag{14}$$

Therefore the exponent n in Eq. (13) is expected to have a minimum at temperatures where the $S(T)$ dependence has a maximum (Fig. 15). To check the validity of the relation $nS=1$ [see Eq. (14)], we have plotted the product nS vs T (Fig. 16), with both parameters determined from the magnetization measurements: S as the normalized flux-creep rate and n as the slope of the $\ln E$ vs $\ln j$ plots (Fig. 14). It turns out that the simple relation $nS=1$, originating from the Faraday law if the E vs j dependence really corresponds to Eq. (13), is fulfilled in the whole range of temperatures $T\leq 60$ K used in our experiments [see Figs. 16(a) and 16(b)]. The typical n values are in the range 25–45 (Fig. 15), which implies the presence of a quite sharp, well-defined critical behavior for the I-V curve on a *picovolt* voltage scale (Fig. 14). The latter is a very low value not so easily achieved in conventional methods of I-V measurements.

Next we would like to turn to the discussion of the anisotropy effects. First of all, we are starting from a remarkable similarity between the $S(T)$ dependences for both $\mathbf{H}\|c$ and $\mathbf{H}\perp c$ orientations [Fig. 13(b)]. There are some reasonable arguments given above for the interpretation of the appearance of the $S(T)$ maximum at low temperatures for the $\mathbf{H}\|c$ orientation. These arguments, however, seem to be quite irrelevant to explain the same $S(T)$ behavior for the $\mathbf{H}\perp c$ orientation. We think that the similarity of the $S(T)$ behavior for $\mathbf{H}\|c$ and $\mathbf{H}\perp c$ [Fig. 13(b)] is directly caused by a small ($\alpha\sim 1°-3°$) misorientation of $\mathbf{H}$ with respect to the exact $\mathbf{H}\perp c$ geometry. Such a misorientation, which seems to be quite realistic in a cryostate without built-in facilities to rotate the sample in the course of measurements at low temperatures, is negligible for weakly anisotropic systems, but may be of vital importance for strongly anisotropic compounds.[76] As it has been shown in Refs. 29–31, at nearly all angles, ex-

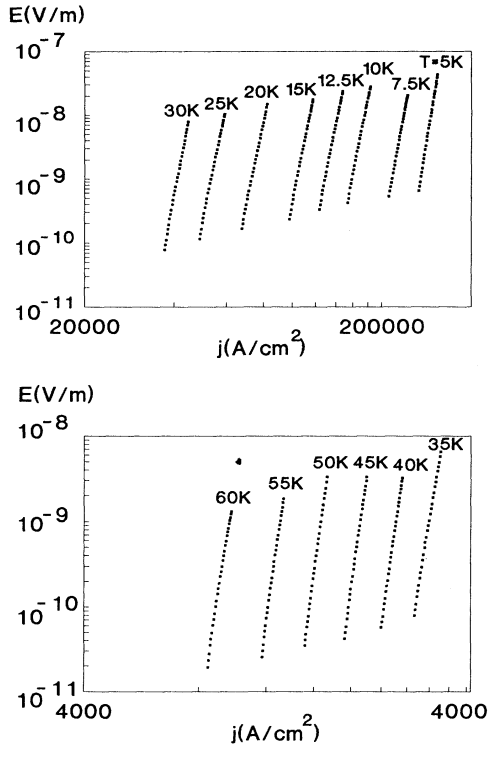

FIG. 14. Current-voltage characteristics of a $Pb_2Sr_2Y_{1-x}Ca_xCu_3O_{8+y}$ single crystal at $\mathbf{H}=0$.

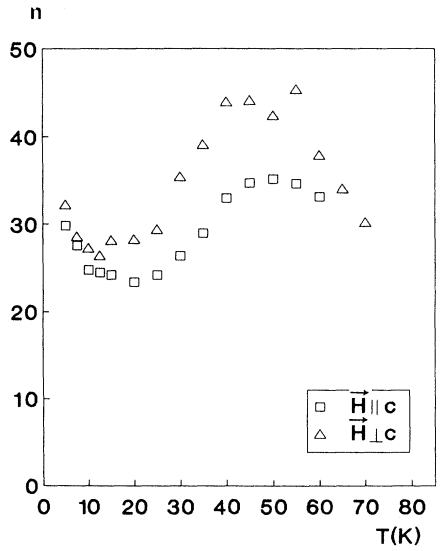

FIG. 15. Temperature dependence of the exponent n in Eq. (13) for $Pb_2Sr_2Y_{1-x}Ca_xCu_3O_{8+y}$, $\mathbf{H}=0$: $\square=\mathbf{H}\|c$, $\triangle=\mathbf{H}\perp c$.

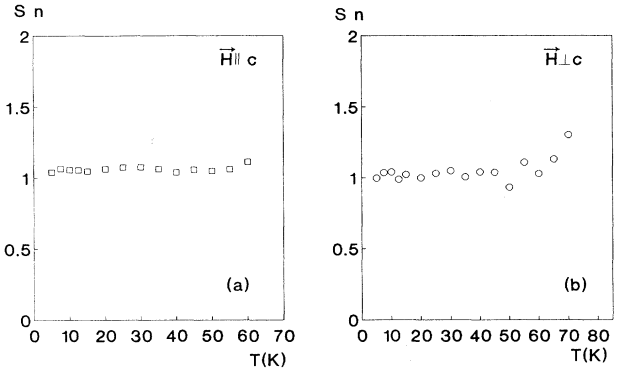

FIG. 16. *Sn* vs T for $Pb_2Sr_2Y_{1-x}Ca_xCu_3O_{8+y}$, $\mathbf{H}=0$: $\square=\mathbf{H}\|c$, $\circ=\mathbf{H}\perp c$.

cept $\alpha\sim\pm1°-3°$ from the exact $\mathbf{H}\perp c$ configuration, the magnetization and its dynamics are determined only by the magnetization component $M^{\|c}$ perpendicular to the CuO_2 layers, which is much larger than the parallel component $M^{\perp c}$ (Ref. 32):

$$M^{\|c}=\frac{\Phi}{16\pi^2 L_{ab}^2\beta(\Theta_v)}\times\left[\ln\left[\frac{\eta\mathbf{H}_{c2}^{\|c}}{B^{\|c}\beta(\Theta_v)}\right]^{1/2}-\frac{1}{2}+\alpha_{3D}\right], \tag{15}$$

$$M^{\perp c}=\frac{\Phi\tan(\Theta_v)}{16\pi^2 L_{ab}^2\Gamma^2\beta(\Theta_v)}\times\left[\ln\left[\frac{\eta\mathbf{H}_{c2}^{\|c}}{B^{\|c}\beta(\Theta)}\right]^{1/2}-\frac{1}{2}+\alpha_{3D}\right], \tag{16}$$

where $\beta(\Theta_v)=[1+\Gamma^{-2}\tan^2(\Theta_v)]^{1/2}$, $\alpha_{3D}\approx0.5$, and $\eta\approx1$.

These are expressions for the *reversible* magnetization in quasi-2D layered superconductors. The ratio $M^{\|c}/M^{\perp c}$ is given by the anisotropy Γ and the angle Θ_v between the vortex lattice and the c axis:

$$\frac{M^{\|c}}{M^{\perp c}}=\frac{\Gamma^2}{\tan(\Theta_v)}.$$

For $\Gamma\sim31$, the difference $M^{\|c}\approx10\ M^{\perp c}$ may be explained by the presence of a very small misorientation angle $\alpha=(\pi/2)-\Theta_v\sim1°$. From this point of view, the striking similarity between $S^{\mathbf{H}\|c}(T)$ and $S^{\mathbf{H}\perp c}(T)$ [Fig. 13(b)] may be easily interpreted as a result of this uncontrollable misorientation, because for tilted fields around $\mathbf{H}\perp c$, the $S^{H\perp c}(T)$ dependence is, in fact, determined by the presence of the small $M^{\|c}(\mathbf{H})$ component and therefore both $S^{\mathbf{H}\perp c}(T)$ and $S^{\mathbf{H}\|c}(T)$ curves should have the same shape, as it is found experimentally [Fig. 13(b)]. Taking this misorientation problem into account, we are concentrating our efforts only on the discussion of the $\mathbf{H}\|c$ orientation.

The same crossover in the pinning regime may also occur if one keeps the temperature constant but varies the magnetic field instead.[59] For the fixed temperatures ($T=30$ K, Fig. 17) we have found a clear indication of a phase transition or a crossover at $\mathbf{H}=\mathbf{H}^{CR}\sim4$ kG ($T=30$ K) and at $\mathbf{H}=\mathbf{H}^{CR}\sim2$ kG ($T=50$ K) (see Fig. 18), where there is a distinct S-shaped anomaly on the I-V curve (Fig. 17). As a result, a kink at $\mathbf{H}=\mathbf{H}^{CR}$ is seen in the n vs $\mathbf{H}$ dependence (Fig. 18). For $T=30$ K the S-shaped anomaly on the I-V dependences, implying the change of the curvature, is clearly observed twice (see Fig. 17) at $\mathbf{H}=4$ kG and $\mathbf{H}=8$ kG. A similar change of the curvature has been reported for $Bi_2Sr_2CaCu_2O_y$ in Ref. 77. Following Fisher *et al.*,[59,60] we propose below a tentative explanation of the variation of the vortex phases as a function of applied field. Firstly, for very strong anisotropy, when

$$\frac{L_c}{L_{ab}}\geq\frac{a_v}{d}=\frac{(\Phi_0/B)^{1/2}}{d}, \tag{17}$$

where $a_v\equiv(\Phi_0/B)^{1/2}$ is a lattice constant, the wavelength of the dominant fluctuations becomes smaller than the interplanar separation d; the system has essentially a 2D character. This is shown in the $\mathbf{H}$-T phase diagram in Fig. 19 above the nearly horizontal dashed line, corre-

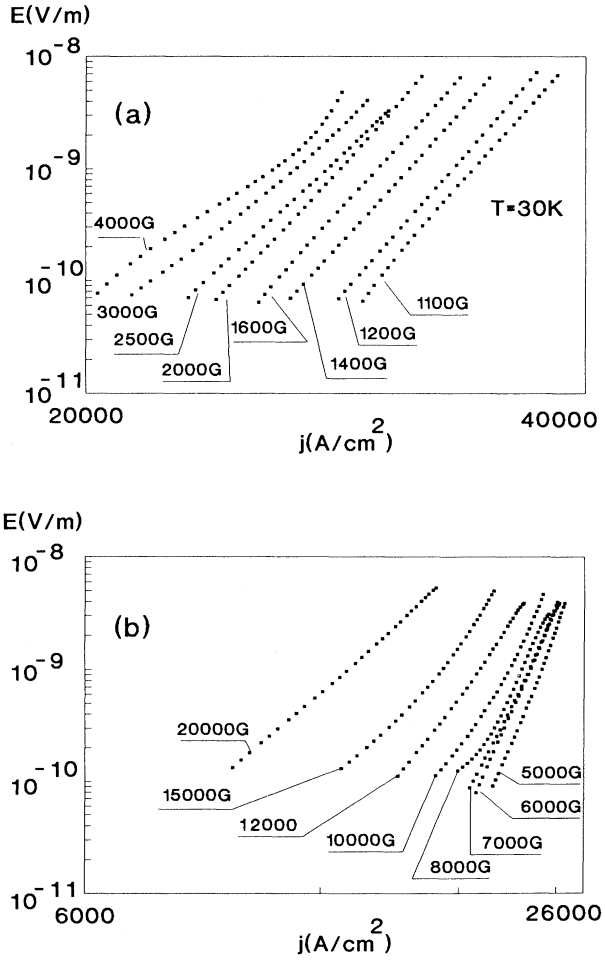

FIG. 17. Current-voltage characteristics of a $Pb_2Sr_2Y_{1-x}Ca_xCu_3O_{8+y}$ single crystal at $T=30$ K for different magnetic fields.

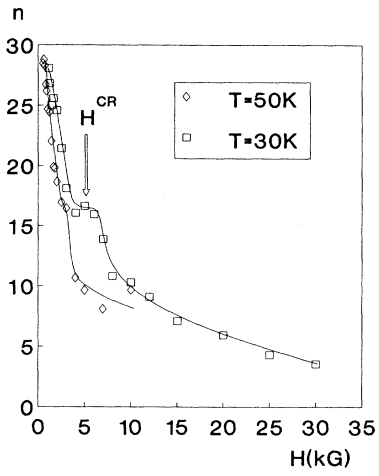

FIG. 18. Field dependence of the exponent n in Eq. (13) for $Pb_2Sr_2Y_{1-x}Ca_xCu_3O_{8+y}$ at $\square = T = 30$ K, $\diamond = T = 50$ K.

sponding to $L_c/L_{ab} = a_v/d$. For this 2D regime the melting line is approximately the same as the Kosterlitz-Thouless-type melting transition T_M^{2D} in a 2D system of logarithmically interacting point vortices in each uncoupled Cu-O layer:[59]

$$T_M^{2D} \approx (1-2)\times 10^{-2} \frac{\Phi_0^2 d}{16\pi^2 L_{ab}^2}$$
$$\approx (20-40\ \text{K}) \left[\frac{1000\ \text{Å}}{L_{ab}(T_M)} \right]^2 \left[\frac{d}{10\ \text{Å}} \right]$$
$$\approx 7-14\ \text{K} . \quad (18)$$

In PSYCCO, with $L_{ab} = 1860$ Å and $d = 12.3$ Å, the crossover line $L_c/L_{ab} = a_v/d$ corresponds to a magnetic field of 10 kG. The T_M^{2D} value, estimated for PSYCCO from Eq. (18), lie in the range 7–14 K. Below T_M^{2D} in magnetic fields $\mathbf{H} > \mathbf{H}^{CR}$, a 2D vortex glass or 2D vortex lattice state should be realized, the former being favored by the presence of disorder. For $\mathbf{H} < \mathbf{H}^{CR}$ the superconducting layers are coupled and the 3D anisotropic behavior takes place with the melting temperature:[59]

$$T_M^{3D} \approx 4c_L^2 \left[\frac{L_{ab}}{L_c} \right] \left[\frac{\Phi_0}{B} \right]^{1/2} \frac{\Phi_0^2}{16\pi^2 L_{ab}^2} , \quad (19)$$

where $c_L \approx 0.15$ is a constant. Thus, for $\mathbf{H} < \mathbf{H}^{CR}$ the melting line follows the T_M^{3D} vs $(\mathbf{H})^{-1/2}$ (see Fig. 19). Below the melting line a 3D vortex glass (or 3D vortex lattice) state is realized, depending upon the strength of the disorder potential present in the system.

Now, coming back to our I-V data (Fig. 17), we may give the following interpretation. The temperatures 30 and 50 K used for the I-V measurements are higher than T_M^{2D} (Fig. 19). For $T > T_M^{2D}$, there are two characteristic fields for which an S-shaped anomaly is seen in the I-V curves; for $T = 30$ K, for example, at $\mathbf{H} \approx 4$ kG and $\mathbf{H} \approx 8$ kG (Fig. 17). The first field seems to correspond to the crossing of the melting line T_M^{3D} [Eq. (19)], whereas the second field may be related to the crossover field $\mathbf{H}^{CR}$ (horizontal dashed line in Fig. 19), corresponding to the 3D-2D reduction of the dimensionality. The value of $\mathbf{H}^{CR}$ is temperature independent if the temperature variation of L [Eq. (18)] is not taken into account. The transition into the 2D vortex liquid phase is also accompanied by the change of the slope of the j_c vs $\mathbf{H}$ (Fig. 12) and S vs $\mathbf{H}$ curves (not shown).

This interpretation of the appearance of the two S-shaped anomalies on the I-V plots is only a qualitative tentative picture, which should be further elaborated on a quantitative level. Of course, it does not necessarily exclude the possible validity of other alternative explanations.

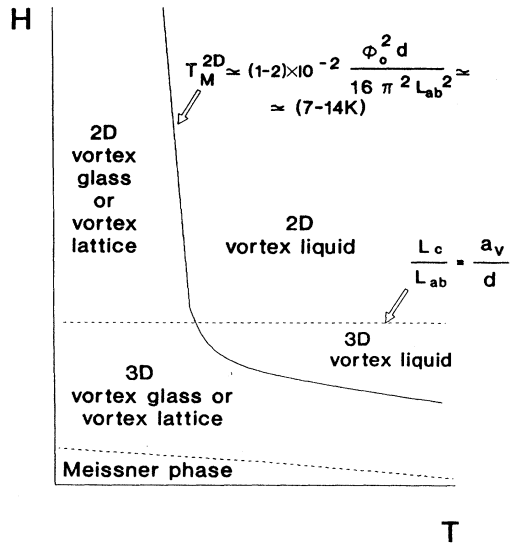

FIG. 19. Schematic phase diagram of a type II layered superconductor as a function of applied magnetic field and temperature.

V. CONCLUSIONS

We have studied temperature dependences of lower critical fields, critical currents, and the flux-creep rate on nearly cube-shaped $0.6\times0.6\times0.5$ mm^3 PSYCCO single crystals for two different field orientations, $\mathbf{H}\|c$ and $\mathbf{H}\perp c$. Lower critical fields $\mathbf{H}_{c1}^{\|c}(T)$ are characterized by an anomalous curvature at low temperatures, which may be interpreted in terms of models which take into account the layered (S-N-S or other types) structure of these oxide superconductors with proximity-induced superconductivity in the layers separating the CuO_2 superconducting planes (Refs. 22–28 and 78,79). The temperature dependences of the critical current $j\mathbf{H}^{\|c}(T)$ and the normalized flux-creep rate $S^{H\|c}(T)$ indicate that with increasing temperature a crossover from the anisotropic 3D to quasi-2D behavior takes place, leading to a strong modification of the pinning mechanism. In comparison with other high-T_c oxides, the anisotropy $\Gamma \equiv (m_c/m_{ab})^{1/2} \approx 31$ is of an intermediate value between YBCO ($\Gamma \approx 5$) and BSCCO ($\Gamma \approx 50-140$). Such a large anisotropy parameter implies

that in order to be sure that the magnetic field **H** is really parallel to the CuO_2 planes, it is necessary to rotate the sample *in situ* in the magnetometer by very small angles about the **H**⊥*c* orientation. Unfortunately we could not do that in our measurements and, as a result, all data given here for **H**⊥*c* are only within ±3° from the exact **H**⊥*c* orientation. This small misorientation may be sufficient to have quite a strong influence of the magnetization component perpendicular to the CuO_2 planes. Because of these reasons the values of the anisotropies of the lower critical fields and critical current given above should be considered only as a lower limit and the real anisotropy might even be higher.

Using current-voltage characteristics in the picovolt range, which were derived from the damping electric field determined by the magnetic-flux-creep rate, we have found that the decoupling of the pancakelike vortices in different CuO_2 planes, occurring at $T \approx T^{CR}$, leads not only to the $j_c(T)$ and $S(T)$ anomalies, but also to the change of the exponent n in the expression [Eq. (13)] relating j to the electric field E.

ACKNOWLEDGMENTS

We thank A. A. Zhukov and V. D. Kuznetsov for helpful discussions. V. Metlushko would like to acknowledge the support by DAAD and DFG SFB 341. V. V. Moshchalkov has benefited from the financial support by the Research Council of the Katholieke Universiteit Leuven.

*Also at Laboratory of High-T_c Superconductivity, Physics Department, Moscow State University, 117234, Moscow, Russia.

[1]R. J. Cava, B. Batlogg, J. J. Krajewski, L. W. Rupp, L. F. Schneemeyer, T. Siegrist, R. B. van Dover, P. Marsh, W. F. Pech, Jr., P. K. Gallagher, S. H. Glarum, J. H. Marshall, R. C. Farrow, J. V. Waszczak, R. Hull, and P. Trevor, Nature (London) **336**, 211 (1988).

[2]M. M. Lukina, V. N. Milov, and V. V. Moshchalkov, Sov. Phys. Supercond. **3**, 2767 (1990).

[3]J. S. Xue, M. Reedyk, Y. P. Lin, C. V. Stager, and J. E. Greedan, Physica C **166**, 29 (1990).

[4]M. Reedyk, C. V. Stager, T. Timusk, J. S. Xue, and J. E. Greedan, Phys. Rev. B **44**, 4539 (1991).

[5]C. Chaillout, O. Chmaissen, J. J. Capponi, T. Fournier, G. J. McIntyre, and M. Marezio, Physica C **175**, 293 (1991).

[6]A. K. Pradhan, S. B. Roy, Chen Changkang, J. W. Hodby, and D. Caplin, Physica C **197**, 22 (1992).

[7]*Magnetic Property Measurement System, Application Notes/Technical Advisories* (Quantum Design, San Diego, 1990), p. 110.

[8]L. D. Landau and E. M. Lifshits, *Electrodynamics of Continuous Media* (Pergamon, London, 1960), p. 417.

[9]A. A. Gippius, V. V. Moshchalkov, and V. V. Pozigun, Fiz. Tverd. Tela (Leningrad) **30**, 765 (1988) [Sov. Phys. Solid State **30**, 438 (1988)].

[10]M. Wacenovsky, H. W. Weber, O. B. Hyun, D. K. Finnemore, and K. Mereiter, Physica C **160**, 55 (1989).

[11]A. P. Malozemoff, L. Krusin-Elbaum, D. C. Cronemeyer, Y. Yeshurun, and F. Holtzberg, Phys. Rev. B **38**, 6490 (1988).

[12]L. Krusin-Elbaum, R. L. Greene, F. Holtzberg, A. P. Malozemoff, and Y. Yeshurun, Phys. Rev. Lett. **62**, 217 (1989).

[13]V. V. Moshchalkov, A. A. Zhukov, V. D. Kuznetsov, V. V. Metlushko, V. I. Voronkova, and V. K. Yanovskii, Solid State Commun. **74**, 1295 (1990).

[14]V. V. Moshchalkov, J. Y. Henry, C. Marin, J. Rossat-Mignod, and J. F. Jacquot, Physica C **175**, 407 (1991).

[15]M. Naito, A. Matsuda, K. Kitazawa, S. Kambe, I. Tanaka, and H. Kojima, Phys. Rev. B **41**, 4823 (1990).

[16]D. E. Farrell, S. Bonham, J. Foster, Y. C. Chang, P. Z. Jiang, K. G. Vandervoort, D. J. Lam, and V. G. Kogan, Phys. Rev. Lett. **63**, 782 (1989).

[17]R. B. van Dover, L. F. Schneemeyer, E. M. Gyorgy, and J. V. Waszczak, Phys. Rev. B **39**, 4800 (1989).

[18]L. A. Gurevich, I. V. Grigor'eva, N. N. Kolesnikov, M. P. Kulakov, V. A. Larkin, and L. Ya. Vinnikov, Physica C **195**, 323 (1992).

[19]D. E. Farrell, C. M. Williams, S. A. Wolf, N. P. Bansal, and V. G. Kogan, Phys. Rev. Lett. **61**, 2805 (1988).

[20]V. Welp, W. K. Kwok, G. W. Crabtree, K. G. Vandervoort, and J. Z. Liu, Phys. Rev. Lett. **62**, 1908 (1989).

[21]G. J. Dolan, F. Holtzberg, C. Field, and T. Dinger, Phys. Rev. Lett. **32**, 2184 (1989).

[22]M. Tachiki, S. Takahasi, F. Steglich, and H. Adrian, Z. Phys. B Condens. Mater. **80**, 161 (1980).

[23]L. N. Bulaevskii, Int. J. Mod. Phys. B **4**, 1849 (1990).

[24]A. I. Buzdin, V. P. Damjanovic, and A. Yu. Simonov, Phys. Rev. B **45**, 7499 (1992).

[25]A. A. Abrikosov, Physica C **182**, 191 (1991).

[26]T. Koyama, N. Takezava, and M. Tachiki, Physica C **168**, 69 (1990).

[27]V. M. Krasnov, Physica C **190**, 357 (1992).

[28]A. A. Golubov and V. M. Krasnov, Physica C **196**, 177 (1992); V. M. Krasnov, V. A. Oboznov, and V. V. Ryazanov, *ibid.* **196**, 335 (1992).

[29]A. V. Balatskii, L. I. Burlachkov, and L. P. Gorkov, Zh. Eksp. Teor. Fiz. **90**, 1478 (1986) [Sov. Phys. JETP **63**, 866 (1986)].

[30]A. I. Buzdin and A. Yu. Simonov, Physica C **175**, 143 (1991).

[31]A. I. Buzdin and A. Yu. Simonov, Physica B **165-166**, 110 (1990).

[32]D. Feinberg, Physica C **194**, 126 (1992).

[33]A. M. Campbell and J. E. Evetts, Adv. Phys. **21**, 199 (1972).

[34]C. P. Bean, Phys. Rev. Lett. **8**, 250 (1962).

[35]C. P. Bean, Rev. Mod. Phys. **36**, 31 (1964).

[36]V. V. Moshchalkov, A. A. Zhukov, L. I. Leoniuk, V. D. Kuznetsov, and V. V. Metlushko, Sov. Phys. Supercond. **2**, 84 (1989).

[37]V. G. Kogan, M. M. Fang, and S. Mitra, Phys. Rev. B **38**, 11 958 (1988).

[38]E. W. Scheidt, C. Hucho, K. Lüders, and V. Müller, Solid State Commun. **71**, 505 (1989).

[39]B. Pumpin, H. Keller, W. Kündig, W. Odermatt, I. M. Sovic, J. W. Schneider, H. Simmler, P. Zimmermann, E. Kaldis, S. Rusiecki, Y. Maeno, and C. Rossel, Phys. Rev. B **42**, 8019 (1990).

[40]S. Mitra, J. H. Cho, W. C. Lee, D. C. Johnston, and V. G. Kogan, Phys. Rev. B **40**, 2674 (1989).

[41]J. R. Thompson, Yang Ren Sun, L. Civale, A. P. Malozemoff, M. W. McElfresh, A. D. Marwick, and F. Holtzberg (unpub-

lished).
[42]A. P. Malozemoff, in *Physical Properties of High Temperature Superconductors,* edited by D. Ginsberg (World Scientific, Singapore, 1989), p. 71.
[43]W. J. Yen, Z. Q. Yu, S. Labroo, and J. Y. Park, Physica C **194**, 141 (1992).
[44]A. A. Zhukov, V. V. Moshchalkov, V. A. Rybachuk, V. A. Murashov, A. Yu. Martynkin, S. W. Moshkin, and I. N. Goncharov, Physica C **185-189**, 2137 (1991).
[45]V. N. Zavaritsky and N. A. Zavaritsky, Physica C **185-189**, 2141 (1991).
[46]A. A. Zhukov, V. V. Moshchalkov, V. A. Rybachuk, V. A. Murashov, and I. N. Goncharov, Zh. Eksp. Teor. Fiz. **53**, 466 (1991) [Sov. Phys. JETP Lett. **53**, 489 (1992)].
[47]D. Neerinck, K. Temst, M. Baert, E. Osquiguil, C. Van Haesendonck, Y. Bruynseraede, A. Gilabert, and I. A. Schuller, Phys. Rev. Lett. **67**, 2577 (1991).
[48]M. Daeumling, J. M. Seuntjens, and C. Larbalestier, Nature (London) **256**, 332 (1990).
[49]S. Senoussi, M. Oussena, G. Collin, and I. A. Campbell, Phys. Rev. B **37**, 9792 (1988).
[50]C. N. Kopylov, A. E. Koshelev, I. F. Schegolev, and T. G. Togonidze, Physica C **170**, 291 (1990).
[51]N. Chikumoto, M. Konczykowski, N. Motohira, K. Kishio, and K. Kitazawa, Physica C **185-189**, 2201 (1991).
[52]V. V. Moshchalkov, A. A. Zhukov, G. T. Karapetrov, V. D. Kusnetov, V. V. Metlushko, V. I. Voronkova, and V. K. Yanovskii, Physica B **169**, 653 (1991).
[53]K. Kadowaki and T. Moshiku, Physica C **195**, 127 (1992).
[54]G. T. Seidler, T. F. Rosenbaum, P. D. Han, D. A. Payne, and B. W. Veal, Physica C **195**, 373 (1992).
[55]A. P. Malozemoff and M. P. A. Fisher, Phys. Rev. B **42**, 6784 (1990).
[56]Y. Xu, M. Suenaga, A. R. Moodenbaugh, and D. O. Welch, Phys. Rev. B **40**, 10 882 (1989).
[57]I. C. Campbell, L. Fruchter, and R. Cabanel, Phys. Rev. B **64**, 1561 (1990).
[58]M. Mittag, M. Rosenberg, A. V. Niculescu, B. Himmerich, and H. Sabrawsky, Physica C **198**, 222 (1992).
[59]D. S. Fisher, M. P. A. Fisher, and D. A. Huse, Phys. Rev. B **43**, 130 (1991).
[60]M. P. A. Fisher, Phys. Rev. Lett. **62**, 1415 (1989).
[61]P. W. Anderson and Y. B. Kim, Rev. Mod. Phys. **36**, 39 (1964).
[62]J. R. Thompson, Y. R. Sun, and F. H. Holtzberg, Phys. Rev. B **44**, 58 (1991).
[63]C. W. Hagen, R. P. Griessen, and E. Salomons, Physica C **157**, 199 (1989).
[64]C. W. Hagen and R. P. Griessen, Phys. Rev. Lett. **62**, 2857 (1989).
[65]E. Zeldov, N. M. Amer, G. Koren, A. Gupta, M. W. McElfresh, and R. J. Gambino, Appl. Phys. Lett. **56**, 680 (1990).
[66]E. Zeldov, N. M. Amer, G. Koren, and A. Gupta, Appl. Phys. Lett. **56**, 1700 (1990).
[67]M. V. Feigel'man, V. B. Geshkenbein, A. I. Larkin, and V. M. Vinokur, Phys. Rev. Lett. **63**, 2303 (1989).
[68]M. V. Feigel'man and V. M. Vinokur, Phys. Rev. B **41**, 8986 (1990).
[69]R. H. Koch, V. Foglietti, W. J. Gallagher, G. Koren, A. Gupta, and M. P. A. Fisher, Phys. Rev. Lett. **63**, 1511 (1989).
[70]G. Ries, H. W. Neumuller, and W. Schmidt, Supercond. Sci. Technol. **5**, S81 (1992).
[71]W. Paul, D. Hu, and Th. Bauman, Physica C **185-189**, 2373 (1991).
[72]J. E. Tkaczyk, R. H. Arendt, M. F. Garbauskas, H. R. Hart, K. W. Lay, and F. E. Luborsky, Phys. Rev. B **45**, 12 506 (1992).
[73]A. A. Zhukov, Solid State Commun. (to be published).
[74]V. V. Metlushko, A. A. Zhukov, V. V. Moshchalkov, V. D. Kuznetsov, M. M. Lukina, and V. N. Milov (to be published).
[75]J. E. Evetts and B. A. Glowacki, Cryogenics **28**, 641 (1988).
[76]S. Senoussi, J. Phys. (Paris) (to be published).
[77]Y. Ando, N. Motohira, K. Kitazawa, J.-I. Takeya, and S. Akita, Phys. Rev. Lett. **67**, 2737 (1991).
[78]A. I. Buzdin, A. Yu. Simonov, and V. P. Damjanovic, Zh. Eksp. Teor. Fiz. **53**, 503 (1991) [Sov. Phys. JETP Lett. **53**, 528 (1991)].
[79]L. N. Bulaevskii and M. V. Zyskin, Phys. Rev. B **42**, 10 230 (1990).